The Astronomical Journal, 154:184 (9pp), 2017 November https://doi.org/10.3847/1538-3881/aa8d69


# Exclusion of Stellar Companions to Exoplanet Host Stars

Justin M. Wittrock[1], Stephen R. Kane[1,2], Elliott P. Horch[3], Steve B. Howell[4], David R. Ciardi[5], and Mark E. Everett[6]
[1] Department of Physics & Astronomy, San Francisco State University, 1600 Holloway Avenue, San Francisco, CA 94132, USA
[2] Department of Earth Sciences, University of California, Riverside, CA 92521, USA
[3] Department of Physics, Southern Connecticut State University, New Haven, CT 06515, USA
[4] NASA Ames Research Center, Moffett Field, CA 94035, USA
[5] NASA Exoplanet Science Institute, Caltech, MS 100-22, 770 South Wilson Avenue, Pasadena, CA 91125, USA
[6] National Optical Astronomy Observatory, 950 N. Cherry Avenue, Tucson, AZ 85719, USA
*Received 2017 July 31; revised 2017 September 14; accepted 2017 September 15; published 2017 October 12*

## Abstract

Given the frequency of stellar multiplicity in the solar neighborhood, it is important to study the impacts this can have on exoplanet properties and orbital dynamics. There have been numerous imaging survey projects established to detect possible low-mass stellar companions to exoplanet host stars. Here, we provide the results from a systematic speckle imaging survey of known exoplanet host stars. In total, 71 stars were observed at 692 and 880 nm bands using the Differential Speckle Survey Instrument at the Gemini-north Observatory. Our results show that all but two of the stars included in this sample have no evidence of stellar companions with luminosities down to the detection and projected separation limits of our instrumentation. The mass–luminosity relationship is used to estimate the maximum mass a stellar companion can have without being detected. These results are used to discuss the potential for further radial velocity follow-up and interpretation of companion signals.

*Key words:* planetary systems – techniques: high angular resolution

## 1. Introduction

The discovery of exoplanets several decades ago (e.g., Latham et al. 1989; Wolszczan & Frail 1992; Latham 2012; Mayor & Queloz 1995) has led to a burgeoning and diverse field of study. A major effort of this work is directed at characterizing the individual exoplanets and their host stars. For example, determining the binarity of the host stars has become a crucial step in understanding exoplanetary systems, as the presence of a binarity companion can have a profound effect on detection methods and formation scenarios. This is particularly important as roughly half of all sun-like stars in the solar neighborhood are part of multiple-star systems (Raghavan et al. 2010; Horch et al. 2014). Indeed, the pursuit of *Kepler* candidates (Everett et al. 2015; Kraus et al. 2016) and Robo-AO observations of radial velocity (RV) exoplanet host stars has significantly contributed to our knowledge of this large rate of stellar multiplicity.

The presence of binary companions can considerably affect stellar measurements intended to discover and/or characterize exoplanets and cause severe blended contamination for transit observations (Cartier et al. 2015; Ciardi et al. 2015; Gilliland et al. 2015). One of the main consequences of this for exoplanets detected by the transit method is the underestimation of their planetary radii determined from the depth of the planetary transit (Ciardi et al. 2015; Furlan & Howell 2017). For systems discovered using the RV method, the presence of stellar companions can manifest as linear trends in the data, the precise origins of which can remain unresolved due to the insufficient time baseline and the $\sin i$ ambiguity of the companion mass interpretation (Crepp et al. 2012; Kane et al. 2014). The range of possible planetary formation scenarios is inhibited by the multiplicity of the stars and can impact such aspects as the orbital stability of the planets (Holman & Wiegert 1999). Furthermore, there has been a noted effect of stellar binarity on masses, orbital periods (Zucker & Mazeh 2002), and eccentricities (Eggenberger et al. 2004) of planets in such binary systems. Consequently, it has become critical for us to establish the multiplicity of exoplanet host stars so that we can be absolutely confident with the resulting interpretation of exoplanet signals and be successful in fully characterizing the overall system properties.

Wittrock et al. (2016) described a survey for exoplanet host star multiplicity and presented the detection of stellar companions to 2 of 71 surveyed exoplanet host stars, HD 2638 and HD 164509. Here, we present the results for the remaining 69 stars of the survey that place significant constraints on the presence of stellar companions to those stars. In Section 2, we discuss the method of detection, the range of targets that were selected for analysis, and the properties of null-detection systems. Section 3 briefly reviews the details of the data reduction and includes sensitivity plots of the observed systems. Section 4 presents the results from the data analysis, and Section 5 provides discussion of further work and concluding remarks.

## 2. Selections and Properties of the Targeted Systems

A large survey project was established to search for stellar companions to a subset of the known RV exoplanet host stars. In total, 71 stars were observed in 2014 July using the Differential Speckle Survey Instrument, or DSSI (Horch et al. 2009); that instrument was stationed at the Gemini-north Observatory at the time of the observations. The stars were selected from the known RV exoplanet host star population where there was no known stellar companion. Two of the stars, HD 2638 and HD 164509, were found to have evidence for bound stellar companions contained in the data (Wittrock et al. 2016). Tables 1 and 2 list the 69 targets from the survey for which no stellar companion was detected. The first table includes spectral types, apparent magnitudes $m_V$, proper motions (denoted as $\mu$), parallaxes, distances, and the number of exoplanets each star hosts, while the second table tallies stellar masses, radii, luminosity, effective temperatures, surface gravity, age, and metallicity. The data within both tables were taken from multiple literature and

**Table 1**
Stellar Properties of RV Exoplanet Host Stars with Null-detections I

| Star | Spectral Type | $m_V^{(33)}$ | $\mu\ \alpha,\ \delta$ (mas yr$^{-1}$)$^{(33)}$ | Parallax (mas)$^{(33)}$ | Distance (pc) | Planets | References |
|---|---|---|---|---|---|---|---|
| BD+14 4559 | K2 V | 9.7768 | 235.80, 1.78 | 20.68 ± 1.24 | 48.36 ± 2.90 | 1 | (25) |
| BD+48 738 | K0 III | 9.14 | 3.7, −6.5 | 2.85 ± 0.00 | 350.88 ± 0.00 | 1 | (10), (28), (36) |
| GJ 581 | M3 V | 10.5759 | −1227.67, −97.78 | 160.91 ± 2.62 | 6.21 ± 0.10 | 3 | (2) |
| GJ 649 | M2 V | 9.7165 | −114.07, −506.26 | 96.67 ± 1.39 | 10.34 ± 0.15 | 2 | (35) |
| GJ 849 | M3 V | 10.3672 | 1130.27, −19.27 | 109.94 ± 2.07 | 9.10 ± 0.17 | 1 | (3) |
| HD 1461 | G3 V | 6.6029 | 416.87, −143.83 | 43.02 ± 0.51 | 23.25 ± 0.28 | 2 | (14) |
| HD 1502 | K0 IV | 8.5196 | 74.64, −18.15 | 6.28 ± 0.75 | 159.24 ± 19.02 | 1 | (6) |
| HD 3651 | K0 V | 6.03 | −461.32, −370.02 | 90.42 ± 0.32 | 11.06 ± 0.04 | 2 | (14) |
| HD 4313 | G5 IV | 7.9939 | −5.14, 6.69 | 7.3 ± 0.76 | 136.99 ± 14.26 | 1 | (6) |
| HD 5319 | K3 IV | 8.2069 | −4.93, −49.66 | 8.74 ± 0.86 | 114.42 ± 11.26 | 2 | (12) |
| HD 5891 | G5 III | 8.2541 | 2.64, −41.89 | 3.98 ± 1.21 | 251.26 ± 76.39 | 1 | (6) |
| HD 6718 | G5 V | 8.5834 | 192.24, 19.77 | 18.23 ± 0.76 | 54.85 ± 2.29 | 1 | (23) |
| HD 7449 | F8 V | 7.6205 | −160.79, −138.95 | 25.69 ± 0.48 | 38.93 ± 0.73 | 2 | (4) |
| HD 8574 | F8 V | 7.2497 | 250.87, −158.06 | 22.44 ± 0.53 | 44.56 ± 1.05 | 1 | (6) |
| HD 9446 | G5 V | 8.5125 | 192.01, −53.99 | 19.1 ± 1.06 | 52.36 ± 2.91 | 2 | (6) |
| HD 10697 | G5 IV | 6.4169 | −44.75, −105.35 | 30.7 ± 0.43 | 32.57 ± 0.46 | 1 | (6) |
| HD 12661 | G6 V | 7.567 | −107.12, −174.69 | 28.61 ± 0.61 | 34.95 ± 0.75 | 2 | (8) |
| HD 13189 | K2 II | 7.6968 | 2.62, 5.32 | 1.78 ± 0.73 | 561.80 ± 230.40 | 1 | (17) |
| HD 13931 | G0 V | 7.7426 | 99.03, −183.19 | 22.61 ± 0.66 | 44.23 ± 1.29 | 1 | (16) |
| HD 16175 | G0 V | 7.4156 | −38.90, −40.37 | 17.28 ± 0.67 | 57.87 ± 2.24 | 1 | (6) |
| HD 16400 | G5 III | 5.8154 | 40.18, −42.91 | 10.81 ± 0.45 | 92.51 ± 3.85 | 1 | (6) |
| HD 16760 | G5 V | 8.8411 | 79.20, −107.49 | 22 ± 2.35 | 45.45 ± 4.86 | 1 | (30) |
| HD 17092 | K0 III | 7.73 | 37.9, −13.6 | 9.2 ± 5.5 | 108.70 ± 64.98 | 1 | (6), (18), (24) |
| HD 136118 | F9 V | 7.0513 | −122.69, 23.72 | 21.47 ± 0.54 | 46.58 ± 1.17 | 1 | (7) |
| HD 136418 | G5 IV | 8.0279 | −19.66, −181.92 | 10.18 ± 0.58 | 98.23 ± 5.60 | 1 | (6) |
| HD 137510 | G0 IV | 6.3856 | −54.91, −5.39 | 24.24 ± 0.51 | 41.25 ± 0.87 | 1 | (5) |
| HD 139357 | K4 III | 6.1335 | −18.32, 1.64 | 8.47 ± 0.3 | 118.06 ± 4.18 | 1 | (6) |
| HD 142245 | K0 IV | 7.6302 | −55.58, −20.82 | 9.13 ± 0.62 | 109.53 ± 7.44 | 1 | (6) |
| HD 143107 | K3 III | 4.2992 | −77.07, −60.61 | 14.73 ± 0.21 | 67.89 ± 0.97 | 1 | (6) |
| HD 143761 | G0 V | 5.5246 | −196.63, −773.02 | 58.02 ± 0.28 | 17.24 ± 0.08 | 2 | (32) |
| HD 145457 | K0 III | 6.7416 | −18.34, 36.89 | 7.98 ± 0.45 | 125.31 ± 7.07 | 1 | (6) |
| HD 145675 | K0 V | 6.7595 | 131.83, −297.54 | 56.91 ± 0.34 | 17.57 ± 0.10 | 1 | (14) |
| HD 149143 | G0 IV | 8.0354 | −9.26, −87.31 | 16.12 ± 0.83 | 62.03 ± 3.19 | 1 | (9) |
| HD 152581 | K0 IV | 8.5372 | 11.49, −15.79 | 5.39 ± 0.96 | 185.53 ± 33.04 | 1 | (6) |
| HD 154345 | G8 V | 6.907 | 123.27, 853.63 | 53.8 ± 0.32 | 18.59 ± 0.11 | 1 | (6) |
| HD 155358 | G0 V | 7.3946 | −222.45, −215.97 | 22.67 ± 0.48 | 44.11 ± 0.93 | 2 | (6) |
| HD 156279 | K0 V | 8.2107 | −1.21, 161.21 | 27.32 ± 0.44 | 36.60 ± 0.59 | 1 | (6) |
| HD 156668 | K3 V | 8.5711 | −71.16, 217.36 | 40.86 ± 0.86 | 24.47 ± 0.52 | 1 | (14) |
| HD 158038 | K2 II | 7.6439 | 48.35, −59.04 | 9.65 ± 0.74 | 103.63 ± 7.95 | 1 | (6) |
| HD 163607 | G5 IV | 8.1487 | −75.74, 120.05 | 14.53 ± 0.46 | 68.82 ± 2.18 | 2 | (11) |
| HD 164922 | G9 V | 7.151 | 389.41, −602.03 | 45.21 ± 0.54 | 22.12 ± 0.26 | 2 | (14) |
| HD 167042 | K1 IV | 6.1356 | 107.94, 247.35 | 19.91 ± 0.26 | 50.23 ± 0.66 | 1 | (20) |
| HD 170693 | K2 III | 4.9835 | 105.83, −27.24 | 10.36 ± 0.2 | 96.53 ± 1.86 | 1 | (6) |
| HD 171028 | G0 IV | 8.31 | −43.8, −13.4 | 9.1 ± 7.8 | 109.89 ± 94.19 | 1 | (6), (18), (27) |
| HD 173416 | G8 III | 6.2114 | 21.11, 58.23 | 7.17 ± 0.28 | 139.47 ± 5.45 | 1 | (6) |
| HD 177830 | K0 IV | 7.3455 | −40.84, −51.75 | 16.94 ± 0.63 | 59.03 ± 2.20 | 2 | (34) |
| HD 180314 | K0 III | 6.7743 | 47.19, 19.71 | 7.61 ± 0.39 | 131.41 ± 6.73 | 1 | (31) |
| HD 187123 | G2 V | 7.9689 | 143.18, −123.91 | 20.72 ± 0.53 | 48.26 ± 1.23 | 2 | (13) |
| HD 190228 | G5 IV | 7.452 | 105.2, −69.82 | 16.23 ± 0.64 | 61.61 ± 2.43 | 1 | (6) |
| HD 192263 | K2.5 V | 7.931 | −61.13, 261.37 | 51.77 ± 0.78 | 19.32 ± 0.29 | 1 | (14) |
| HD 197037 | F7 V | 6.9226 | −62.47, −220.96 | 30.93 ± 0.38 | 32.33 ± 0.40 | 1 | (26) |
| HD 199665 | G6 III | 5.6682 | −48.75, −34.43 | 13.28 ± 0.31 | 75.30 ± 1.76 | 1 | (6) |
| HD 200964 | K0 IV | 6.6386 | 94.99, 50.47 | 13.85 ± 0.52 | 72.20 ± 2.71 | 2 | (29) |
| HD 206610 | K0 IV | 8.5066 | 2.35, 2.34 | 5.16 ± 0.95 | 193.80 ± 35.68 | 1 | (6) |
| HD 208527 | M1 III | 6.4842 | 2.00, 15.30 | 2.48 ± 0.38 | 403.23 ± 61.78 | 1 | (22) |
| HD 210277 | G8 V | 6.6823 | 85.07, −449.74 | 46.38 ± 0.48 | 21.56 ± 0.22 | 1 | (14) |
| HD 210702 | K1 IV | 6.0932 | −3.15, −18.02 | 18.2 ± 0.39 | 54.95 ± 1.18 | 1 | (19) |
| HD 217014 | G2 V | 5.5865 | 207.25, 60.34 | 64.07 ± 0.38 | 15.61 ± 0.09 | 1 | (15) |
| HD 217107 | G8 IV | 6.3124 | −6.35, −15.80 | 50.36 ± 0.38 | 19.86 ± 0.15 | 2 | (14) |
| HD 217786 | F9 V | 7.9103 | −88.78, −170.13 | 18.23 ± 0.72 | 54.85 ± 2.17 | 1 | (6) |
| HD 218566 | K3 V | 8.7269 | 632.56, −97.02 | 35.02 ± 1.14 | 28.56 ± 0.93 | 1 | (6) |
| HD 219828 | G0 IV | 8.1795 | −4.15, 4.14 | 13.83 ± 0.74 | 72.31 ± 3.87 | 2 | (6) |
| HD 220074 | M2 III | 6.4885 | 7.68, −5.43 | 3.08 ± 0.43 | 324.68 ± 45.33 | 1 | (21) |
| HD 220773 | F9 V | 7.2306 | 26.90, −222.87 | 19.65 ± 0.65 | 50.89 ± 1.68 | 1 | (26) |

**Table 1**
(Continued)

| Star | Spectral Type | $m_V^{(33)}$ | $\mu\ \alpha,\ \delta$ (mas yr$^{-1}$)$^{(33)}$ | Parallax (mas)$^{(33)}$ | Distance (pc) | Planets | References |
|---|---|---|---|---|---|---|---|
| HD 221345 | K0 III | 5.3841 | 286.72, −84.22 | 12.63 ± 0.27 | 79.18 ± 1.69 | 1 | (6) |
| HD 222155 | G2 V | 7.2445 | 195.33, −117.13 | 20.38 ± 0.62 | 49.07 ± 1.49 | 1 | (1) |
| HD 231701 | F8 V | 9.0929 | 63.85, 16.46 | 8.44 ± 1.05 | 118.48 ± 14.74 | 1 | (6) |
| HD 240210 | K3 III | 8.33 | 18.0, 7.9 | 7 ± 2.6 | 142.86 ± 53.06 | 1 | (18), (25) |
| HD 240237 | K2 III | 8.2959 | −0.74, −5.13 | 0.19 ± 0.72 | 5263.16 ± 19944.60 | 1 | (10) |

**References.** (1) Boisse et al. (2012), (2) Bonfils et al. (2005), (3) Bonfils et al. (2013), (4) Dumusque et al. (2011), (5) Endl et al. (2004), (6) ESA (1997), (7) Fischer et al. (2002), (8) Fischer et al. (2003), (9) Fischer et al. (2006), (10) Gettel et al. (2012), (11) Giguere et al. (2012), (12) Giguere et al. (2015), (13) Gray et al. (2001), (14) Gray et al. (2003), (15) Gray et al. (2006), (16) Grenier et al. (1999), (17) Hatzes et al. (2005), (18) Hog et al. (2000), (19) Johnson et al. (2007), (20) Johnson et al. (2008), (21) Kidger et al. (2003), (22) Lee et al. (2013), (23) Naef et al. (2010), (24) Niedzielski et al. (2007), (25) Niedzielski et al. (2009), (26) Robertson et al. (2012), (27) Santos et al. (2007), (28) Santos et al. (2013), (29) Santos et al. (2015), (30) Sato et al. (2009), (31) Sato et al. (2010), (32) van Belle & von Braun (2009), (33) van Leeuwen (2007), (34) Vogt et al. (2000), (35) von Braun et al. (2014), (36) Zacharias (2004).

**Table 2**
Stellar Properties of RV Exoplanet Host Stars with Null-detection II

| Name | $M_\star$ ($M_\odot$) | $R_\star$ ($R_\odot$) | $L_\star$ ($L_\odot$) | $T_e$ (K) | log $g$ (cm s$^{-2}$) | Age (Gyr) | [Fe/H] | References |
|---|---|---|---|---|---|---|---|---|
| BD+14 4559 | 0.82 ± 0.02 | 0.78 ± 0.02 | 0.32 ± 0.01 | 4948 ± 25 | 4.57 ± 0.03 | 6.9 ± 4.2 | 0.17 ± 0.06 | (3), (15) |
| BD+48 738 | 0.74 ± 0.39 | 11 ± 1 | 49 ± 37.2 | 4519 ± 30 | 2.51 ± 0.03 | ... | −0.24 ± 0.02 | (5), (8) |
| GJ 581 | 0.306 ± 0.011 | 0.299 ± 0.007 | 0.01146 ± 0.00061 | 3457 ± 22 | 4.96 ± 0.25 | 9.44 ± 0.58 | −0.15 ± 0.08 | (12), (15) |
| GJ 649 | 0.527 ± 0.013 | 0.495 ± 0.012 | 0.04308 ± 0.00276 | 3741 ± 39 | 4.76 ± 0.12 | 9.42 ± 0.57 | 0.03 ± 0.08 | (12), (15) |
| GJ 849 | 0.482 ± 0.048 | 0.47 ± 0.018 | 0.03079 ± 0.00315 | 3530 ± 60 | 4.8 ± 0.14 | 9.4 ± 0.58 | 0.37 ± 0.08 | (12), (15) |
| HD 1461 | 1.07 ± 0.01 | 1.08 ± 0.01 | 1.2 ± 0.01 | 5807 ± 20 | 4.39 ± 0.01 | 4 ± 0.7 | 0.16 ± 0.03 | (3), (11) |
| HD 1502 | 1.46 ± 0.04 | 4.5 ± 0.1 | 11.5 ± 0.2 | 5006 ± 25 | 3.29 ± 0.02 | 3 ± 0.3 | −0.01 ± 0.06 | (3), (8) |
| HD 3651 | 0.88 ± 0.02 | 0.86 ± 0.01 | 0.51 ± 0.01 | 5271 ± 26 | 4.51 ± 0.02 | 6.9 ± 2.8 | 0.19 ± 0.02 | (3), (11) |
| HD 4313 | 1.49 ± 0.04 | 5.2 ± 0.1 | 14 ± 0.2 | 4920 ± 21 | 3.18 ± 0.02 | 3 ± 0.3 | 0.11 ± 0.07 | (3), (8) |
| HD 5319 | 1.2 ± 0.1 | 4 ± 0.1 | 8.2 ± 0.1 | 4888 ± 39 | 3.3 ± 0.04 | 6.1 ± 1.4 | 0.15 ± 0.03 | (3), (6) |
| HD 5891 | 1.1 ± 0.1 | 9.1 ± 0.2 | 39.1 ± 0.4 | 4796 ± 41 | 2.57 ± 0.05 | 5.7 ± 1.5 | −0.37 ± 0.04 | (3), (8) |
| HD 6718 | 0.97 ± 0.02 | 1.02 ± 0.03 | 1.06 ± 0.02 | 5805 ± 46 | 4.4 ± 0.03 | 6.2 ± 2 | −0.11 ± 0.05 | (1), (3) |
| HD 7449 | 1.05 ± 0.02 | 1.02 ± 0.02 | 1.26 ± 0.02 | 6060 ± 42 | 4.44 ± 0.02 | 2.2 ± 1.3 | −0.11 ± 0.01 | (3), (15) |
| HD 8574 | 1.17 ± 0.02 | 1.38 ± 0.04 | 2.35 ± 0.04 | 6092 ± 56 | 4.22 ± 0.03 | 4.4 ± 0.6 | 0.06 ± 0.07 | (3), (15) |
| HD 9446 | 1.04 ± 0.03 | 1.03 ± 0.03 | 1.06 ± 0.03 | 5790 ± 45 | 4.43 ± 0.03 | 3.7 ± 2 | 0.09 ± 0.05 | (3), (15) |
| HD 10697 | 1.12 ± 0.01 | 1.7 ± 0.1 | 2.8 ± 0.04 | 5674 ± 93 | 4 ± 0.03 | 7.5 ± 0.4 | 0.15 ± 0.04 | (3), (8) |
| HD 12661 | 1.09 ± 0.01 | 1.08 ± 0.01 | 1.13 ± 0.01 | 5714 ± 22 | 4.4 ± 0.01 | 3.3 ± 0.6 | 0.36 ± 0.05 | (3), (15) |
| HD 13189 | 1.08 ± 0.17 | ⋯ | ⋯ | 4228 ± 242 | 2.09 ± 0.61 | ⋯ | −0.5 ± 0.14 | (15) |
| HD 13931 | 1.07 ± 0.02 | 1.17 ± 0.03 | 1.48 ± 0.03 | 5902 ± 52 | 4.33 ± 0.03 | 5.3 ± 1.3 | 0.07 ± 0.01 | (3), (17) |
| HD 16175 | 1.3 ± 0.05 | 1.69 ± 0.03 | 3.35 ± 0.02 | 6009 ± 44 | 4.09 ± 0.02 | 4.1 ± 0.8 | 0.37 ± 0.03 | (3), (16) |
| HD 16400 | 1.4 ± 0.1 | 11.2 ± 0.2 | 59.8 ± 0.4 | 4799 ± 24 | 2.49 ± 0.03 | 3.2 ± 0.5 | 0 ± 0.04 | (3), (8) |
| HD 16760 | 0.93 ± 0.01 | 0.835 ± 0.005 | 0.58 ± 0.002 | 5518 ± 11 | 4.56 ± 0.01 | 1.3 ± 0.9 | 0 ± 0.02 | (2), (14) |
| HD 17092 | 1.246 ± 0.179 | 10.439 ± 1.31 | 43.64 ± 11.23 | 4596 ± 65 | 2.45 ± 0.17 | 5.58 ± 2.669 | 0.05 ± 0.04 | (16) |
| HD 136118 | 1.15 ± 0.03 | 1.54 ± 0.03 | 3.03 ± 0.01 | 6135 ± 37 | 4.12 ± 0.03 | 5.3 ± 0.6 | −0.01 ± 0.053 | (2), (7) |
| HD 136418 | 1.2 ± 0.1 | 3.5 ± 0.1 | 6.9 ± 0.1 | 4997 ± 40 | 3.43 ± 0.04 | 5 ± 1 | −0.09 ± 0.03 | (3), (16) |
| HD 137510 | 1.41 ± 0.01 | 1.91 ± 0.03 | 4.33 ± 0.01 | 6032 ± 44 | 4.02 ± 0.02 | 3.1 ± 0.2 | 0.29 ± 0.12 | (2), (9) |
| HD 139357 | 1.1 ± 0.1 | 14.4 ± 0.4 | 73.5 ± 1.3 | 4454 ± 39 | 2.2 ± 0.1 | 7.2 ± 1.8 | 0.19 ± 0.05 | (3), (16) |
| HD 142245 | 1.52 ± 0.05 | 5.2 ± 0.1 | 13.1 ± 0.2 | 4831 ± 28 | 3.19 ± 0.03 | 3.1 ± 0.3 | 0.23 ± 0.03 | (3), (15) |
| HD 143107 | 1.44 ± 0.18 | 21 ± 0 | 151 ± 0 | 4436 ± 56 | 1.94 ± 0.15 | 1.74 ± 0.37 | −0.22 ± 0.03 | (13), (15) |
| HD 143761 | 0.889 ± 0.03 | 1.3617 ± 0.0262 | 1.706 ± 0.042 | 5627 ± 54 | 4.121 ± 0.018 | 9.1 ± 1 | −0.31 ± 0.05 | (2), (4) |
| HD 145457 | 1.5 ± 0.1 | 9.4 ± 0.2 | 41 ± 1 | 4772 ± 45 | 2.66 ± 0.05 | 2.8 ± 0.6 | −0.13 ± 0.03 | (3), (16) |
| HD 145675 | 0.97 ± 0.01 | 0.93 ± 0.01 | 0.61 ± 0.01 | 5313 ± 18 | 4.48 ± 0.02 | 4.6 ± 1.5 | 0.5 ± 0.06 | (3), (11) |
| HD 149143 | 1.21 ± 0.03 | 1.5 ± 0.1 | 2.2 ± 0.1 | 5792 ± 58 | 4.17 ± 0.03 | 4.8 ± 0.8 | 0.45 ± 0.07 | (3), (15) |
| HD 152581 | 1 ± 0.1 | 5.4 ± 0.1 | 16.1 ± 0.2 | 4991 ± 45 | 3 ± 0.1 | 7.2 ± 2 | −0.3 ± 0.02 | (3), (16) |
| HD 154345 | 0.9 ± 0.01 | 0.85 ± 0.01 | 0.62 ± 0.002 | 5557 ± 15 | 4.53 ± 0.01 | 4.1 ± 1.2 | −0.09 ± 0.02 | (3), (11) |
| HD 155358 | 1.1 ± 0.1 | 1.36 ± 0.03 | 2.11 ± 0.02 | 5966 ± 53 | 4.2 ± 0.04 | 1.9 ± 4.5 | −0.62 ± 0.02 | (3), (15) |
| HD 156279 | 0.93 ± 0.02 | 0.94 ± 0.02 | 0.7 ± 0.01 | 5449 ± 31 | 4.45 ± 0.03 | 7.4 ± 2.2 | 0.14 ± 0.01 | (3), (15) |
| HD 156668 | 0.75 ± 0.01 | 0.73 ± 0.01 | 0.27 ± 0.01 | 4857 ± 18 | 4.58 ± 0.01 | 10.2 ± 2.8 | −0.04 ± 0.05 | (3), (15) |
| HD 158038 | 1.5 ± 0.1 | 4.9 ± 0.1 | 11.9 ± 0.1 | 4839 ± 29 | 3.23 ± 0.03 | 3.2 ± 0.4 | 0.16 ± 0.05 | (3), (16) |
| HD 163607 | 1.1 ± 0.02 | 1.8 ± 0.1 | 2.6 ± 0.1 | 5508 ± 15 | 3.98 ± 0.01 | 8.3 ± 0.5 | 0.22 ± 0.02 | (3), (16) |
| HD 164922 | 0.874 ± 0.012 | 0.999 ± 0.017 | 0.703 ± 0.017 | 5293 ± 32 | 4.387 ± 0.014 | 7.9 ± 2.7 | 0.16 ± 0.05 | (3), (4) |
| HD 167042 | 1.46 ± 0.05 | 4.4 ± 0.1 | 10.7 ± 0.1 | 4989 ± 32 | 3.31 ± 0.03 | 3.1 ± 0.3 | −0.01 ± 0.06 | (3), (8) |
| HD 170693 | 1.1 ± 0.1 | 20.6 ± 0.6 | 145 ± 3 | 4414 ± 40 | 1.8 ± 0.1 | 6.5 ± 1.7 | −0.41 ± 0.03 | (3), (16) |
| HD 171028 | 0.98 ± 0.04 | 2 ± 0.2 | 3.9 ± 0.5 | 5771 ± 46 | 3.84 ± 0.03 | 8.2 ± 1.1 | −0.47 ± 0.02 | (3), (8) |
| HD 173416 | 1.8 ± 0.2 | 13 ± 0.3 | 80 ± 2 | 4790 ± 37 | 2.5 ± 0.1 | 1.8 ± 0.7 | −0.15 ± 0.03 | (3), (16) |

**Table 2**
(Continued)

| Name | $M_\star$ ($M_\odot$) | $R_\star$ ($R_\odot$) | $L_\star$ ($L_\odot$) | $T_e$ (K) | log $g$ (cm s$^{-2}$) | Age (Gyr) | [Fe/H] | References |
|---|---|---|---|---|---|---|---|---|
| HD 177830 | 1.1 ± 0.1 | 3.4 ± 0.1 | 5.3 ± 0.1 | 4735 ± 31 | 3.39 ± 0.04 | 10.2 ± 1.7 | 0.09 ± 0.04 | (3), (8) |
| HD 180314 | 2.3 ± 0.1 | 8.7 ± 0.3 | 40 ± 1 | 4946 ± 55 | 2.92 ± 0.05 | 0.9 ± 0.2 | 0.11 ± 0.04 | (3), (16) |
| HD 187123 | 1.06 ± 0.02 | 1.17 ± 0.03 | 1.44 ± 0.02 | 5853 ± 53 | 4.32 ± 0.03 | 5.6 ± 1.3 | 0.13 ± 0.03 | (3), (15) |
| HD 190228 | 1.18 ± 0.04 | 2.4 ± 0.1 | 4.4 ± 0.2 | 5352 ± 30 | 3.73 ± 0.02 | 5 ± 0.5 | −0.24 ± 0.06 | (2), (8) |
| HD 192263 | 0.78 ± 0.02 | 0.73 ± 0.01 | 0.3 ± 0.01 | 4980 ± 20 | 4.59 ± 0.02 | 5.9 ± 3.9 | −0.01 ± 0.05 | (3), (11) |
| HD 197037 | 1.063 ± 0.022 | 1.105 ± 0.023 | 1.568 ± 0.074 | 6150 ± 34 | 4.37 ± 0.04 | 3.408 ± 0.924 | −0.16 ± 0.03 | (16) |
| HD 199665 | 2.1 ± 0.1 | 7.8 ± 0.3 | 35 ± 1 | 5037 ± 57 | 2.98 ± 0.04 | 1 ± 0.1 | 0.1 ± 0.02 | (3), (8) |
| HD 200964 | 1.4 ± 0.1 | 4.7 ± 0.1 | 12.8 ± 0.2 | 5059 ± 34 | 3.23 ± 0.03 | 3.1 ± 0.4 | −0.16 ± 0.03 | (3), (8) |
| HD 206610 | 1.51 ± 0.05 | 6 ± 0.2 | 18 ± 1 | 4836 ± 30 | 3.05 ± 0.03 | 3 ± 0.3 | 0.09 ± 0.05 | (3), (8) |
| HD 208527 | 1.6 ± 0.4 | 51.1 ± 8.3 | 621.3 ± 205.8 | 4035 ± 65 | 1.4 ± 0.2 | 2 ± 1.3 | −0.09 ± 0.16 | (10) |
| HD 210277 | 0.96 ± 0.02 | 1.05 ± 0.03 | 0.92 ± 0.03 | 5530 ± 40 | 4.37 ± 0.03 | 8.8 ± 1.9 | 0.26 ± 0.02 | (3), (11) |
| HD 210702 | 1.47 ± 0.04 | 4.9 ± 0.1 | 12.9 ± 0.1 | 4946 ± 25 | 3.22 ± 0.02 | 3.1 ± 0.3 | −0.05 ± 0.04 | (3), (8) |
| HD 217014 | 1.09 ± 0.02 | 1.13 ± 0.03 | 1.34 ± 0.03 | 5857 ± 39 | 4.37 ± 0.02 | 3.8 ± 1.1 | 0.2 ± 0.02 | (3), (11) |
| HD 217107 | 1.08 ± 0.01 | 1.11 ± 0.02 | 1.14 ± 0.01 | 5676 ± 31 | 4.38 ± 0.02 | 4.2 ± 1 | 0.37 ± 0.02 | (3), (11) |
| HD 217786 | 1.03 ± 0.02 | 1.27 ± 0.04 | 1.93 ± 0.04 | 6031 ± 55 | 4.23 ± 0.03 | 6.8 ± 0.9 | −0.14 ± 0.01 | (3), (15) |
| HD 218566 | 0.8 ± 0.01 | 0.77 ± 0.02 | 0.3 ± 0.01 | 4880 ± 16 | 4.57 ± 0.02 | 8 ± 3.1 | 0.17 ± 0.04 | (3), (15) |
| HD 219828 | 1.2 ± 0.04 | 1.58 ± 0.04 | 2.74 ± 0.03 | 5921 ± 53 | 4.11 ± 0.03 | 5.2 ± 0.8 | 0.16 ± 0.04 | (3), (8) |
| HD 220074 | 1.2 ± 0.3 | 49.7 ± 9.5 | 531.6 ± 211.7 | 3935 ± 110 | 1.1 ± 0.2 | 4.5 ± 2.8 | −0.25 ± 0.25 | (10) |
| HD 220773 | 1.154 ± 0.003 | 1.73 ± 0.02 | 3.16 ± 0.01 | 5852 ± 26 | 4.02 ± 0.01 | 6.3 ± 0.1 | 0.11 ± 0.03 | (3), (15) |
| HD 221345 | 1.2 ± 0.2 | 11 ± 0.3 | 56 ± 1 | 4775 ± 49 | 2.4 ± 0.1 | 5.6 ± 3 | −0.29 ± 0.03 | (3), (16) |
| HD 222155 | 1.05 ± 0.01 | 1.7 ± 0.1 | 2.9 ± 0.1 | 5814 ± 43 | 4 ± 0.01 | 8.1 ± 0.4 | −0.09 ± 0.02 | (3), (16) |
| HD 231701 | 1.23 ± 0.01 | 1.48 ± 0.05 | 2.94 ± 0.05 | 6211 ± 71 | 4.18 ± 0.03 | 3.7 ± 0.5 | 0.04 ± 0.02 | (3), (15) |
| HD 240210 | 1.241 ± 0.238 | 19.293 ± 4.399 | 115.9 ± 53.5 | 4316 ± 78 | 1.91 ± 0.21 | 5.085 ± 3.089 | −0.14 ± 0.03 | (16) |
| HD 240237 | 0.614 ± 0.076 | 0.587 ± 0.274 | 0.1183 ± 0.1109 | 4422 ± 101 | 1.69 ± 0.24 | 4.42 ± 4.007 | −0.24 ± 0.06 | (16) |

**References.** (1) Bensby et al. (2014), (2) Bonfanti et al. (2015), (3) Bonfanti et al. (2016), (4) Fulton et al. (2016), (5) Gettel et al. (2012), (6) Giguere et al. (2015), (7) Gonzalez & Laws (2007), (8) Jofre et al. (2015), (9) Kang et al. (2011), (10) Lee et al. (2013), (11) Maldonado et al. (2015), (12) Mann et al. (2015), (13) Massarotti et al. (2008), (14) McCarthy & Wilhelm (2014), (15) Santos et al. (2013), (16) Sousa et al. (2015), (17) Spina et al. (2016).

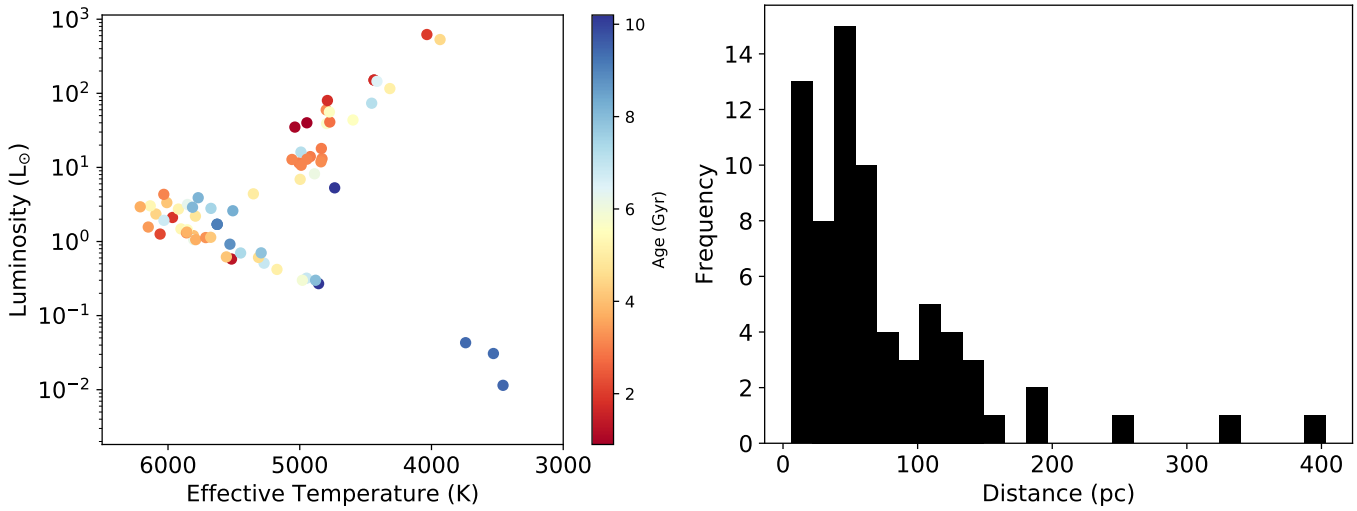


**Figure 1.** Left: H–R diagram of the stars included in the survey, where the color bar indicates the stellar age in Gyr. Right: histogram of distances to the surveyed stars. The data from these plots are from Tables 1 and 2.

exoplanet databases (see reference section). The DSSI used two different filters, 692 and 880 nm, to acquire the speckle images of those targets. The 692 nm filter has FWHM of 40 nm, and the 880 nm filter has FWHM of 50 nm. All images were reduced using a data reduction pipeline, the details of which are provided in Section 3. Afterward, the images were examined by eye and also using the speckle reduced data plots for any companion source appearing next to the target.

Figure 1 showcases the Hertzsprung–Russell (H–R) diagram and distance histogram of the survey using the data from Tables 1 and 2. BD+48 738 and HD 13189 were excluded because their luminosity and/or age data are unavailable, and HD 240237 was excluded due to its extremely large distance of 5300 pc. As described by Wittrock et al. (2016), this is a magnitude-limited survey that targets the brightest of known exoplanet host stars, and so the sample consists mostly of relatively nearby dwarf stars with a peak in the distance distribution of ∼50 pc. The large distances of the giant stars results in a small angular separation sensitivity for detecting stellar companions.

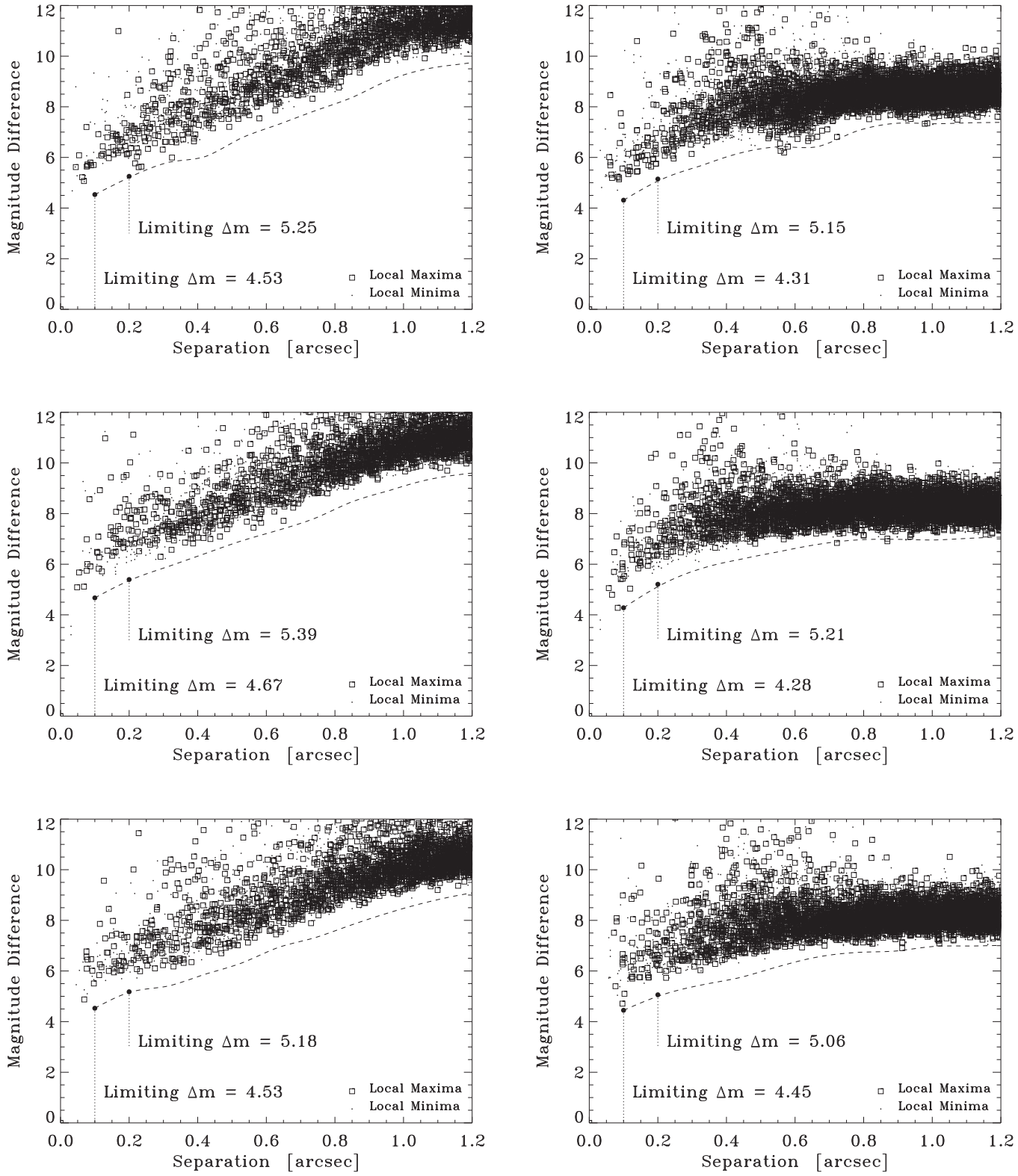


**Figure 2.** Limiting magnitude plots for selected targets. Left and right columns are sensitivity plots at 692 nm and 880 nm, respectively. Each plot shows the limiting magnitude (difference between local maxima and minima) as a function of apparent separation from a given target in units of arcsec. The dashed line is a cubic spline interpolation of the 5$\sigma$ detection limit. Both plots were generated from the corresponding DSSI images. The Gemini diffraction limits are 0.″021 and 0.″027 at 692 nm and 880 nm, respectively.

## 3. Observations and Data Reduction

The details on the process undergone to obtain the final reconstructed images is provided in the previous paper (Wittrock et al. 2016) and with greater depth in Horch et al. (2012, 2015) but will be summarized here. The DSSI obtains the raw speckle data and stores it as FITS data cubes containing 1000 single short-exposure frames, where each frame is a 256 × 256-pixel image centered on the target. The plate scales

**Table 3**
Limiting Magnitudes

| Name | Exclusion Radius (au) | | $5\sigma$ $\Delta m$ Limit (692 nm) | | $5\sigma$ $\Delta m$ Limit (880 nm) | | $m - M$ | Max Mass ($M_\odot$) | |
|---|---|---|---|---|---|---|---|---|---|
| | Inner | Outer | 0.″1 | 0.″2 | 0.″1 | 0.″2 | | 692 nm | 880 nm |
| BD+14 4559 | 2.42 | 67.70 | 3.92 | 4.32 | 3.93 | 4.62 | 3.42 | 0.26 | 0.26 |
| BD+48 738 | 17.54 | 491.23 | 3.09 | 5.01 | 3.72 | 4.74 | 7.73 | 1.35 | 1.14 |
| GJ 581 | 0.31 | 8.70 | 4.36 | 5.14 | 4.29 | 5.23 | −1.03 | 0.09 | 0.09 |
| GJ 649 | 0.52 | 14.48 | 3.40 | 4.23 | 3.39 | 4.27 | 0.07 | 0.17 | 0.17 |
| GJ 849 | 0.45 | 12.73 | 4.01 | 4.55 | 3.95 | 4.55 | −0.21 | 0.13 | 0.13 |
| HD 1461 | 1.16 | 32.54 | 3.21 | 4.15 | 3.54 | 4.89 | 1.83 | 0.45 | 0.41 |
| HD 1502 | 7.96 | 222.93 | 4.44 | 5.20 | 4.29 | 4.97 | 6.01 | 0.63 | 0.65 |
| HD 2638 | 2.50 | 69.90 | 4.45 | 4.96 | 3.83 | 4.63 | 3.49 | 0.24 | 0.28 |
| HD 3651 | 0.55 | 15.48 | 4.53 | 5.25 | 4.31 | 5.15 | 0.22 | 0.25 | 0.27 |
| HD 4313 | 6.85 | 191.78 | 4.67 | 5.39 | 4.28 | 5.21 | 5.68 | 0.62 | 0.69 |
| HD 5319 | 5.72 | 160.18 | 4.09 | 5.30 | 4.15 | 5.23 | 5.29 | 0.62 | 0.61 |
| HD 5891 | 12.56 | 351.76 | 4.41 | 5.37 | 4.43 | 5.31 | 7.00 | 0.89 | 0.89 |
| HD 6718 | 2.74 | 76.80 | 4.32 | 4.80 | 4.20 | 4.95 | 3.70 | 0.33 | 0.34 |
| HD 7449 | 1.95 | 54.50 | 4.28 | 4.91 | 4.21 | 4.80 | 2.95 | 0.35 | 0.35 |
| HD 8574 | 2.23 | 62.39 | 4.53 | 5.18 | 4.45 | 5.06 | 3.24 | 0.39 | 0.40 |
| HD 9446 | 2.62 | 73.30 | 4.75 | 5.24 | 4.49 | 5.08 | 3.59 | 0.29 | 0.31 |
| HD 10697 | 1.63 | 45.60 | 4.50 | 5.20 | 4.10 | 4.80 | 2.56 | 0.41 | 0.46 |
| HD 12661 | 1.75 | 48.93 | 4.51 | 5.22 | 4.16 | 5.15 | 2.72 | 0.32 | 0.35 |
| HD 13189 | 28.09 | 786.52 | 4.03 | 5.33 | 3.73 | 4.87 | 8.75 | 0.00 | 0.00 |
| HD 13931 | 2.21 | 61.92 | 3.55 | 5.05 | 3.84 | 4.97 | 3.23 | 0.44 | 0.41 |
| HD 16175 | 2.89 | 81.02 | 3.44 | 5.03 | 4.08 | 5.30 | 3.81 | 0.57 | 0.48 |
| HD 16400 | 4.63 | 129.51 | 2.28 | 4.22 | 2.99 | 3.66 | 4.83 | 1.77 | 1.47 |
| HD 16760 | 2.27 | 63.64 | 3.93 | 4.99 | 3.81 | 4.77 | 3.29 | 0.30 | 0.31 |
| HD 17092 | 5.43 | 152.17 | 3.11 | 4.64 | 4.27 | 5.07 | 5.18 | 1.30 | 0.96 |
| HD 136118 | 2.33 | 65.21 | 4.49 | 5.37 | 4.07 | 5.07 | 3.34 | 0.42 | 0.47 |
| HD 136418 | 4.91 | 137.52 | 4.03 | 4.99 | 3.59 | 4.52 | 4.96 | 0.60 | 0.67 |
| HD 137510 | 2.06 | 57.76 | 4.27 | 4.92 | 3.84 | 4.83 | 3.08 | 0.49 | 0.55 |
| HD 139357 | 5.90 | 165.29 | 2.83 | 4.73 | 3.74 | 4.65 | 5.36 | 1.62 | 1.28 |
| HD 142245 | 5.48 | 153.34 | 4.30 | 5.01 | 4.73 | 5.30 | 5.20 | 0.67 | 0.60 |
| HD 143107 | 3.39 | 95.04 | 4.33 | 5.32 | 4.05 | 5.25 | 4.16 | 1.34 | 1.44 |
| HD 143107 | 3.39 | 95.04 | 4.44 | 5.19 | 4.26 | 5.20 | 4.16 | 1.30 | 1.37 |
| HD 143761 | 0.86 | 24.13 | 2.65 | 3.66 | 4.17 | 4.96 | 1.18 | 0.58 | 0.39 |
| HD 143761 | 0.86 | 24.13 | 4.09 | 4.81 | 3.72 | 4.68 | 1.18 | 0.40 | 0.44 |
| HD 143761 | 0.86 | 24.13 | 4.42 | 4.95 | 4.33 | 5.19 | 1.18 | 0.36 | 0.37 |
| HD 145457 | 6.27 | 175.44 | 4.44 | 4.96 | 4.62 | 5.15 | 5.49 | 0.90 | 0.86 |
| HD 145675 | 0.88 | 24.60 | 4.30 | 5.13 | 4.18 | 5.34 | 1.22 | 0.28 | 0.29 |
| HD 149143 | 3.10 | 86.85 | 4.39 | 4.96 | 4.12 | 5.09 | 3.96 | 0.39 | 0.42 |
| HD 152581 | 9.28 | 259.74 | 4.52 | 5.09 | 4.53 | 5.05 | 6.34 | 0.67 | 0.67 |
| HD 154345 | 0.93 | 26.02 | 3.70 | 4.96 | 3.60 | 4.72 | 1.35 | 0.33 | 0.34 |
| HD 155358 | 2.21 | 61.76 | 3.37 | 4.75 | 3.34 | 4.55 | 3.22 | 0.51 | 0.51 |
| HD 156279 | 1.83 | 51.24 | 2.93 | 4.53 | 4.22 | 4.86 | 2.82 | 0.42 | 0.30 |
| HD 156668 | 1.22 | 34.26 | 3.90 | 5.18 | 3.53 | 4.71 | 1.94 | 0.25 | 0.27 |
| HD 158038 | 5.18 | 145.08 | 4.48 | 5.24 | 4.22 | 5.07 | 5.08 | 0.62 | 0.67 |
| HD 163607 | 3.44 | 96.35 | 3.30 | 4.51 | 4.40 | 4.95 | 4.19 | 0.55 | 0.41 |
| HD 164509 | 2.62 | 73.41 | 3.90 | 4.15 | 4.00 | 4.52 | 3.60 | 0.39 | 0.38 |
| HD 164922 | 1.11 | 30.97 | 3.69 | 4.88 | 3.64 | 4.76 | 1.72 | 0.34 | 0.35 |
| HD 167042 | 2.51 | 70.32 | 3.22 | 3.84 | 4.29 | 5.15 | 3.50 | 0.84 | 0.64 |
| HD 170693 | 4.83 | 135.14 | 2.58 | 4.05 | 2.74 | 3.84 | 4.92 | 2.10 | 2.02 |
| HD 171028 | 5.49 | 153.85 | 3.84 | 4.09 | 4.00 | 4.45 | 5.20 | 0.54 | 0.52 |
| HD 173416 | 6.97 | 195.26 | 3.33 | 3.51 | 3.75 | 4.01 | 5.72 | 1.45 | 1.30 |
| HD 177830 | 2.95 | 82.64 | 3.13 | 3.23 | 4.05 | 4.29 | 3.86 | 0.71 | 0.56 |
| HD 180314 | 6.57 | 183.97 | 3.23 | 3.48 | 4.13 | 4.46 | 5.59 | 1.23 | 0.97 |
| HD 187123 | 2.41 | 67.57 | 3.89 | 3.98 | 3.93 | 4.34 | 3.42 | 0.40 | 0.39 |
| HD 190228 | 3.08 | 86.26 | 3.82 | 4.03 | 4.07 | 4.56 | 3.95 | 0.56 | 0.52 |
| HD 192263 | 0.97 | 27.04 | 1.85 | 3.55 | 3.34 | 4.21 | 1.43 | 0.44 | 0.29 |
| HD 197037 | 1.62 | 45.26 | 4.07 | 4.25 | 4.05 | 4.63 | 2.55 | 0.39 | 0.39 |
| HD 199665 | 3.77 | 105.42 | 3.82 | 4.30 | 3.89 | 4.48 | 4.38 | 1.01 | 0.99 |
| HD 200964 | 3.61 | 101.08 | 1.97 | 3.18 | 3.70 | 4.60 | 4.29 | 1.23 | 0.78 |
| HD 206610 | 9.69 | 271.32 | 4.15 | 4.60 | 4.52 | 5.00 | 6.44 | 0.77 | 0.69 |
| HD 208527 | 20.16 | 564.52 | 4.02 | 4.17 | 3.84 | 4.10 | 8.03 | 2.18 | 2.29 |
| HD 210277 | 1.08 | 30.19 | 4.14 | 4.27 | 4.42 | 5.05 | 1.67 | 0.33 | 0.30 |
| HD 210702 | 2.75 | 76.92 | 4.12 | 4.54 | 4.48 | 4.74 | 3.70 | 0.70 | 0.64 |

**Table 3**
(Continued)

| Name | Exclusion Radius (au) | | $5\sigma$ $\Delta m$ Limit (692 nm) | | $5\sigma$ $\Delta m$ Limit (880 nm) | | $m - M$ | Max Mass ($M_\odot$) | |
|---|---|---|---|---|---|---|---|---|---|
| | Inner | Outer | 0.″1 | 0.″2 | 0.″1 | 0.″2 | | 692 nm | 880 nm |
| HD 217014 | 0.78 | 21.85 | 4.07 | 4.60 | 3.49 | 4.24 | 0.97 | 0.37 | 0.43 |
| HD 217107 | 0.99 | 27.80 | 4.23 | 4.88 | 4.35 | 5.27 | 1.49 | 0.34 | 0.33 |
| HD 217786 | 2.74 | 76.80 | 4.51 | 5.20 | 4.44 | 5.16 | 3.70 | 0.37 | 0.37 |
| HD 218566 | 1.43 | 39.98 | 4.41 | 5.19 | 4.20 | 5.18 | 2.28 | 0.22 | 0.23 |
| HD 219828 | 3.62 | 101.23 | 4.41 | 5.19 | 4.31 | 5.12 | 4.30 | 0.42 | 0.43 |
| HD 220074 | 16.23 | 454.55 | 3.21 | 3.89 | 4.31 | 4.67 | 7.56 | 2.58 | 1.93 |
| HD 220773 | 2.54 | 71.25 | 4.25 | 4.94 | 4.22 | 4.87 | 3.53 | 0.45 | 0.46 |
| HD 221345 | 3.96 | 110.85 | 4.43 | 5.00 | 3.93 | 4.87 | 4.49 | 0.98 | 1.12 |
| HD 222155 | 2.45 | 68.69 | 3.91 | 4.15 | 4.24 | 4.61 | 3.45 | 0.48 | 0.44 |
| HD 231701 | 5.92 | 165.88 | 4.10 | 4.18 | 4.10 | 4.31 | 5.37 | 0.46 | 0.46 |
| HD 240210 | 7.14 | 200.00 | 3.72 | 4.13 | 3.72 | 4.25 | 5.77 | 1.46 | 1.46 |
| HD 240237 | 263.16 | 7368.42 | 3.30 | 4.65 | 4.52 | 5.18 | 13.61 | 0.23 | 0.17 |

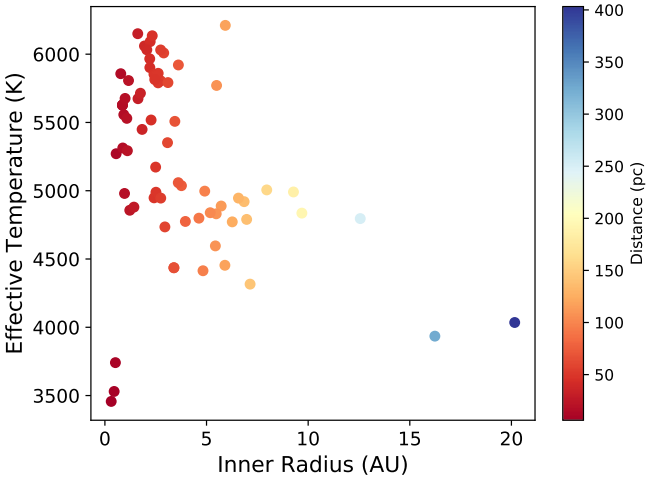


**Figure 3.** Inner radius versus effective temperature of the targets. The color bar represents the distance in pc.

for the observing run at Gemini-north were 0.01081 arcsec/pixel and 0.01120 arcsec/pixel for the 692 nm and 880 nm channels, respectively. The frames are bias-subtracted, auto-correlated, and then summed. The result is then Fourier transformed to retrieve the spatial frequency power spectrum of both the science target and a known unresolved point source standard. Afterward, the science target's power spectrum is divided by that of the point source to deconvolve the effects of the speckle transfer function and obtain a diffraction-limited estimate of the true power spectrum of the object. For the raw data frames, the image bispectrum of each frame has been created (more details on this process have been described in Lohmann et al. 1983). The relaxation algorithm of Meng et al. (1990) is then applied to calculate the phase of the object's Fourier transform. This result is then added with the square root of the deconvolved power spectrum to arrive at an estimate of the object's Fourier transform. Next, it is multiplied with a Gaussian low-pass filter of FWHM width equal to the telescope's diffraction limit. Lastly, we inverse-Fourier-transform the result to obtain the final reconstructed image.

With the reconstructed images in hand, we can use the method from Horch et al. (2011) to obtain a detection limit curve with respect to angular separation from the primary star. The average and standard deviation of the maxima inside annuli are computed to guide our estimation of the $5\sigma$ detection limit, which is the mean value plus five times the standard deviation. These values are in units of magnitude difference. The DSSI's diffraction limit on Gemini-north (0.″022 at 692 nm and 0.″027 at 880 nm) constrains the angular range of annuli from 0.″1 to ∼1.″2, and we arbitrarily chose an increment of 0.″1 for the annuli. Afterward, we employed a cubic spline interpolation to achieve a smooth detection limit curve at all separations in between the two extreme limits. The sensitivity plots with these curves for some targets are listed in Figure 2. The construction of these sensitivity plots are described in more detail by Howell et al. (2011).

## 4. Results

Even though the remaining systems have not yielded the discovery of a stellar companion like those of HD 2638 and HD 164509 (Wittrock et al. 2016), such results nevertheless provide an important contribution to the stellar companion survey. Given that the field-of-view of the images is 2.″8 × 2.″8, a null-detection implies that the system contains no stellar companions down to the sensitivity limit of the observation and within the projected size of the field-of-view. For example, one such system for which we do not detect a stellar companion and is relatively nearby (∼17 pc) is 14 Her (HD 145675). Wittenmyer et al. (2007) proposed a second exoplanet, 14 Her c, with a semimajor axis of 6.9 au and very low eccentricity of 0.02 ± 0.06. Our non-detection of a stellar companion around 14 Her out to ∼25 au (see Table 3) indicates that the observed signal for the outer body is highly likely to be caused by a planetary body.

Table 3 includes the inner and outer exclusion radii, limiting magnitudes at 0.″1 and 0.″2, the distance moduli, and the maximum stellar mass of a hypothetical companion for each target, including HD 2638 and HD 164509 from Wittrock et al. (2016). The exclusion radii are the range of physical separations from the host star that are observable within the Gemini DSSI's field-of-view. The exclusion radii and the distance moduli are calculated using the stellar distances provided in Table 1. The minimum angular separation is constrained by Gemini's diffraction limits of about 0.″022 at 692 nm and 0.″027 at 880 nm and is 0.″05. As mentioned before, the maximum angular separation is 1.″2, which provides a constraint on the outer exclusion radius. Thus, the exclusion

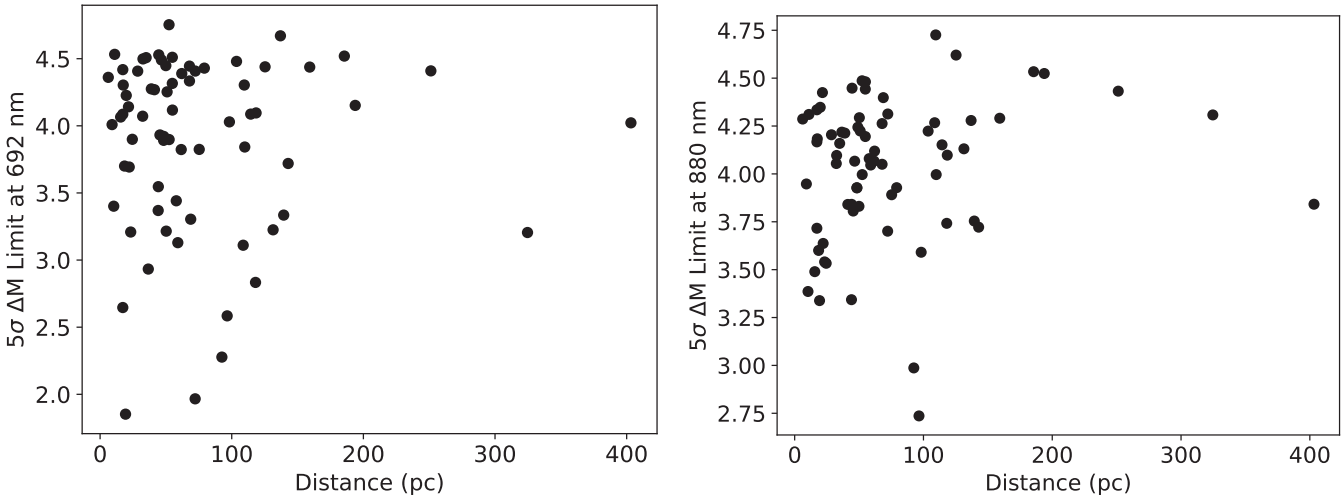


**Figure 4.** Correlations between host star distances and limiting magnitude at 0.″1. The plot on the left is at 692 nm while the one on the right is at 880 nm.

radii provide a region where stellar companions with certain spectral types may be excluded. Therefore, the last two columns tell us the maximum mass a stellar companion can have before becoming detectable via DSSI within the exclusion region. These masses were calculated using a simple mass–luminosity relationship of $(L_\star/L_\odot) = (M_\star/M_\odot)^{3.5}$ (Kuiper 1938) and the given limiting magnitudes at both 692 and 880 nm.

We constructed three plots, shown in Figures 3 and 4, using the information from Table 3. Figure 3 shows some correlation between the inner exclusion radius and effective temperature of the targets, with tight clusters at or below 5 au. The large inner exclusion radius for some of the cooler stars represents the giant stars in the sample, as verified by the distance indicators. The plots displayed in Figure 4 show that the limiting magnitudes of our observations are largely consistent between the two passbands used of 692 and 880 nm. As for Figure 1, BD+48 738, HD 13189, and HD 240237 were excluded from the plots (see Section 2).

## 5. Conclusion

Detection of stellar companions to exoplanet host stars is now relatively common. Their discovery, or lack of it, are of beneficial contributions to the structure of stellar systems, as the presence of a stellar companion significantly influences the orbital dynamics and models for formation processes. For planets discovered using the RV technique, the search for stellar companions plays a major role in the correct interpretation of residual RV trends present in the data. Furthermore, determining if any of the known exoplanet host stars are single, binary, or multiple systems is absolutely essential in avoiding situations where a gas giant would be mistaken for a terrestrial or even an Earth-like planet.

Our DSSI survey monitored 71 stars for which 2 were detected to have stellar companions (Wittrock et al. 2016), and the remaining 69 show no evidence of stellar companions within the 2.″8 × 2.″8 field-of-view and above the instrument's sensitivity limit. This increases the probability that remaining detected objects in the RV data, if any, are planetary bodies if not extremely low-mass stars or brown dwarfs. An example of this is the 14 Her system, for which the partial phase coverage of the RV signal detected by Wittenmyer et al. (2007) is better explained by a planetary body rather than stellar, as our exclusion range out to ∼25 au completely encompasses the postulated semimajor axis of the proposed 14 Her c. The exclusion radii listed in Table 3 provide a physical range of separations from each star within which any future RV detection of objects gravitationally bound to these stars may now be more closely associated with a planetary object.

The authors would like to thank the referee for providing feedback that improved the quality of the paper. This work is based on observations obtained at the Gemini Observatory, which is operated by the Association of Universities for Research in Astronomy, Inc., under a cooperative agreement with the NSF on behalf of the Gemini partnership: the National Science Foundation (United States), the National Research Council (Canada), CONICYT (Chile), the Australian Research Council (Australia), Ministério da Ciência, Tecnologia e Inovação (Brazil) and Ministerio de Ciencia, Tecnología e Innovación Productiva (Argentina). This research has made use of the NASA Exoplanet Archive, which is operated by the California Institute of Technology, under contract with the National Aeronautics and Space Administration under the Exoplanet Exploration Program. The results reported herein benefited from collaborations and/or information exchange within NASA's Nexus for Exoplanet System Science (NExSS) research coordination network sponsored by NASA's Science Mission Directorate.

## ORCID iDs

Stephen R. Kane https://orcid.org/0000-0002-7084-0529
Elliott P. Horch https://orcid.org/0000-0003-2159-1463
Steve B. Howell https://orcid.org/0000-0002-2532-2853
Mark E. Everett https://orcid.org/0000-0002-0885-7215

## References

Bensby, T., Feltzing, S., & Oey, M. 2014, A&A, 562, A71
Boisse, I., Pepe, F., Perrier, C., et al. 2012, A&A, 545, A55
Bonfanti, A., Ortolani, S., & Nascimbeni, V. 2016, A&A, 585, A5
Bonfanti, A., Ortolani, S., Piotto, G., & Nascimbeni, V. 2015, A&A, 575, A18
Bonfils, X., Delfosse, X., Udry, S., et al. 2013, A&A, 549, A109
Bonfils, X., Forveille, T., Delfosse, X., et al. 2005, A&A, 443, L15
Cartier, K. M. S., Gilliland, R. L., Wright, J. T., & Ciardi, D. R. 2015, ApJ, 804, 97
Ciardi, D. R., Beichman, C. A., Horch, E. P., & Howell, S. B. 2015, ApJ, 805, 16

Crepp, J. R., Johnson, J. A., Howard, A. W., et al. 2012, ApJ, 761, 39
Dumusque, X., Lovis, C., Segransan, D., et al. 2011, A&A, 535, A55
Eggenberger, A., Udry, S., & Mayor, M. 2004, A&A, 417, 353
Endl, M., Hatzes, A. P., Cochran, W. D., et al. 2004, ApJ, 611, 1121
ESA 1997, The Hipparcos and Tycho Catalogues (Noordwijk: ESA)
Everett, M. E., Barclay, T., Ciardi, D. R., et al. 2015, AJ, 149, 55
Fischer, D., Laughlin, G., Marcy, G., et al. 2006, ApJ, 637, 1094
Fischer, D., Marcy, G., Butler, R., et al. 2003, ApJ, 586, 1394
Fischer, D. A., Marcy, G. W., Butler, R. P., et al. 2002, PASP, 114, 529
Fulton, B. J., Howard, A. W., Weiss, L. M., et al. 2016, ApJ, 830, 46
Furlan, E., & Howell, S. B. 2017, AJ, 154, 66
Gettel, S., Wolszczan, A., Niedzielski, A., et al. 2012, ApJ, 745, 10
Giguere, M. J., Fischer, D. A., Howard, A. W., et al. 2012, ApJ, 744, 4
Giguere, M. J., Fischer, D. A., Payne, M. J., et al. 2015, ApJ, 799, 89
Gilliland, R. L., Cartier, K. M. S., Adams, E. R., et al. 2015, AJ, 149, 24
Gonzalez, G., & Laws, C. 2007, MNRAS, 378, 1141
Gray, R., Corbally, C., Garrison, R., et al. 2003, AJ, 126, 2048
Gray, R., Corbally, C., Garrison, R., et al. 2006, AJ, 132, 161
Gray, R., Napier, M., & Winkler, L. 2001, AJ, 121, 2148
Grenier, S., Baylac, M.-O., Rolland, L., et al. 1999, A&AS, 137, 451
Hatzes, A., Guenther, E., Endl, M., et al. 2005, A&A, 437, 743
Hog, E., Fabricius, C., & Makarov, V. V. 2000, A&A, 355, L27
Holman, M. J., & Wiegert, P. A. 1999, AJ, 117, 621
Horch, E. P., Gomez, S. C., Sherry, W. H., et al. 2011, AJ, 141, 45
Horch, E. P., Howell, S. B., Everett, M. E., et al. 2012, AJ, 144, 165
Horch, E. P., Howell, S. B., Everett, M. E., & Ciardi, D. R. 2014, ApJ, 795, 60
Horch, E. P., van Altena, W. F., Demarque, P., et al. 2015, AJ, 149, 151
Horch, E. P., Veillette, D. R., Baena, G., et al. 2009, AJ, 137, 5057
Howell, S. B., Everett, M. E., Sherry, W., Horch, E., & Ciardi, D. R. 2011, AJ, 142, 19
Jofre, E., Petrucci, R., Saffe, C., et al. 2015, A&A, 574, 46
Johnson, J., Fischer, D., Marcy, G., et al. 2007, ApJ, 665, 785
Johnson, J., Marcy, G., Fischer, D., et al. 2008, ApJ, 675, 784
Kane, S. R., Howell, S. B., Horch, E. P., et al. 2014, ApJ, 785, 93
Kang, W., Lee, S-G., & Kim, K.-M. 2011, ApJ, 736, 87
Kidger, M., Gonzalez-Perez, J., & Martin-Luis, F. 2003, RMxAC, 16, 287
Kraus, A. L., Ireland, M. J., Huber, D., Mann, A. W., & Dupuy, T. J. 2016, AJ, 152, 8
Kuiper, G. P. 1938, ApJ, 88, 472
Latham, D. W. 2012, NewAR, 56, 16
Latham, D. W., Stefanik, R. P., Mazeh, T., Mayor, M., & Burki, G. 1989, Natur, 339, 38
Lee, B.-C., Han, I., & Park, M.-G. 2013, A&A, 549, A2
Lohmann, A. W., Weigelt, G., & Wirnitzer, B. 1983, ApOpt, 22, 4028
Maldonado, J., Eiroa, C., Villaver, E., et al. 2015, A&A, 579, A20
Mann, A., Feiden, G., Gaidos, E., et al. 2015, ApJ, 804, 64
Massarotti, A., Latham, D. W., Stefanik, R. P., & Fogel, J. 2008, AJ, 135, 209
Mayor, M., & Queloz, D. 1995, Natur, 378, 355
McCarthy, K., & Wilhelm, R. 2014, AJ, 148, 70
Meng, J., Aitken, G. J. M., Hege, E. K., & Morgan, J. S. 1990, JOSAA, 7, 1243
Naef, D., Mayor, M., Lo Curto, G., et al. 2010, A&A, 523, A15
Niedzielski, A., Konacki, M., Wolszczan, A., et al. 2007, ApJ, 669, 1354
Niedzielski, A., Nowak, G., Adamów, M., & Wolszczan, A. 2009, ApJ, 707, 768
Raghavan, D., McAlister, H. A., Henry, T. J., et al. 2010, ApJS, 190, 1
Robertson, P., Endl, M., Cochran, W., et al. 2012, ApJ, 749, 39
Santos, N., Adibekyan, V., Mordasini, C., et al. 2015, A&A, 580, L13
Santos, N., Mayor, M., Bouchy, F., et al. 2007, A&A, 474, 647
Santos, N., Sousa, S., Mortier, A., et al. 2013, A&A, 556A, 150
Sato, B., Fischer, D., Ida, S., et al. 2009, ApJ, 703, 671
Sato, B., Omiya, M., Liu, Y., et al. 2010, PASJ, 62, 1063
Sousa, S., Santos, N., Mortier, A., et al. 2015, A&A, 576, A94
Spina, L., Melendez, J., & Ramirez, I. 2016, A&A, 585, A152
van Belle, G., & von Braun, K. 2009, ApJ, 694, 1085
van Leeuwen, F. 2007, A&A, 474, 653
Vogt, S., Marcy, G., Butler, R., & Apps, K. 2000, ApJ, 536, 902
von Braun, K., Boyajian, T. S., van Belle, G. T., et al. 2014, MNRAS, 438, 2413
Wittenmyer, R. A., Endl, M., & Cochran, W. D. 2007, ApJ, 654, 625
Wittrock, J. M., Kane, S. R., Horch, E. P., et al. 2016, AJ, 152, 149
Wolszczan, A., & Frail, D. A. 1992, Natur, 355, 145
Zacharias, N. 2004, AN, 325, 631
Zucker, S., & Mazeh, T. 2002, ApJL, 568, L113